

The Verwey Transition in Magnetite

David Mertens
Physics 569, ESM

Abstract

The historical development and theories explaining the Verwey transition in Magnetite are discussed. An overview of current experimental work is included. Also examined are multiple charge ordering theories and more sophisticated considerations of Jahn-Teller effects which attempt to explain this long-standing problem in strongly-correlated electron systems.

1 Introduction

Magnetite is the name given to the crystalline solid Fe_3O_4 . It is black in color and has a bit of a sheen to it. It is an oxidized state of Iron and as such is a fairly abundant mineral. In fact the first magnetic materials known to civilization were composed largely of magnetite and other iron oxides; the relation between the words *magnet* and *magnetite* is not coincidental[1].

Given the length of time the material has been known to humans, it is only recently - 65 years ago - that a so-called metal-insulator transition was discovered at around 120K [2]. Despite numerous attempts, a definitive model that explains both the electronic and crystal structure below the transition has been elusive.

The first model to explain the transition was posed by its experimental discoverer about eight years after the initial findings were published[3]. The transition was soon shown to be more complicated than researchers initially thought when evidence of structural changes were published [5].

Magnetite has been studied with nearly every experimental apparatus applicable to solid-state research including x-ray, neutron, and electron scattering, transport, magnetic, and heat capacity measurements, and Mossbauer, NMR, and electronic spectroscopy [6]. It has also suffered a plethora of theoretical excursions including band structure calculations [7] and, more recently, local spin density approximation along with dynamical mean field theory (LSDA+DMFT) [8].

In the study of the topic, some believe that the electronic transition is primary and understanding it will lead to the observed structural transition when the proper spatial elements are added to the theory. On the other hand, some believe that the spatial transition is primary and causes the electronic transition as a consequence.

I chose to write about the Verwey transition in magnetite because I had previously worked with the material experimentally. However, I never really delved into the literature as much as I would have liked and this gave me an opportunity to do just that. I think it is an interesting problem to study because magnetite is such a simple, durable, and fairly ubiquitous material and yet we do not understand how it works in certain temperature regimes. Developing a strong theory to explain strongly-correlated electron systems is an important step in solid-state physics that I expect would lead to numerous applications, especially since magnetite exhibits strong magnetic and semiconductor properties.

2 The Structure of Magnetite

2.1 Above the Transition [1, 9]

The chemical unit for magnetite is Fe_3O_4 , but the crystallographic unit cell is composed of eight such formula units: 24 Iron atoms and 32 Oxygen atoms. Magnetite is ordered in what is called an inverse spinel, a diagram of which is in figure 2.1 on the following page.¹ The spinel (and inverse spinel) unit cells are simple cubic cells. An Iron atom can be in one of two distinct nearest-neighbor arrangements: the A sites are those locations that have nearest neighbors that form a tetrahedron; the B sites are those that are neighbored in an octahedral arrangement.

Magnetite has two different Iron atom valencies: Fe^{2+} and Fe^{3+} . In a normal spinel, the twice-valent atoms would occupy the tetrahedral (A) sites and the thrice-valent atoms would occupy the octahedral (B) sites. In an inverse spinel, the tetrahedral (A) sites are filled by Fe^{3+} atoms and the octahedral (B) sites are filled by an even mix of Fe^{2+} and Fe^{3+} atoms. To reflect this structure, the chemical formula is sometimes written as $Fe^{3+} [Fe^{3+}, Fe^{2+}] O_4$.

¹Whether or not charge-ordering occurs below the transition (strongly implied by this diagram) is the topic of this discussion. Still, the order helps give a sense of the distinction between the two sites.

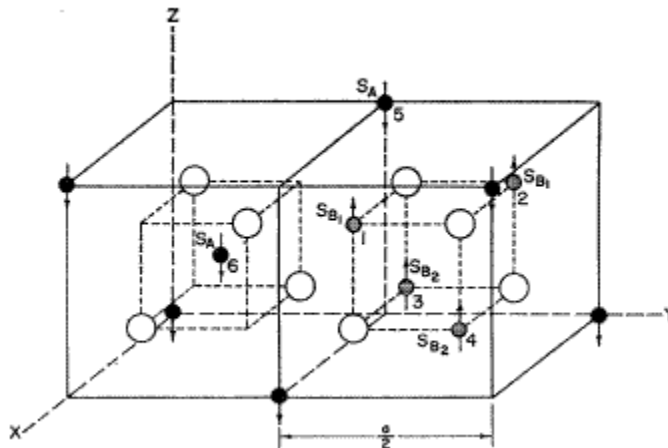


Figure 1: from [9]. “One quarter of the unit cell for ordered inverse spinel. One cation site of each variety is labeled. The open circles represent oxygen sites.” This is an image of an inverse spinel structure taken from Glasser. To construct the entire unit cell, consider the image shown to be constructed to two cubes α and β ; fill the space such that the faces of any α cube directly adjoin only β cubes, and vice versa.

2.2 Below the Transition [4]

In addition to resistivity changes at the transition, magnetite also undergoes a slight crystallographic distortion. The resulting cubic structure requires a larger, monoclinic unit cell to describe it and contains 32 formula units (compared to the eight formula units required for the inverse spinel). A diagram showing the distortions can be found in figure 2.2 on the next page.

As the diagram indicates, the ‘top’ and ‘bottom’ planes of the cube remain parallel to the original cubic faces, but the top gets translated a slight amount. The distortion is very small and less complicated space groups can be used to approximate the structure in calculations.

One of the greatest technical difficulties in studying magnetite in the monoclinic phase is the presence of twinning. Unless it is synthetically manufactured, a single solid piece of magnetite at room temperature is likely to be composed of multiple crystals. The crystals are made distinct by the axes of the unit cells: for example, the c axis of one such crystal might differ from the c axis of another crystal by 5° – it would appear that one is growing out of the other.

As we proceed through the transition from above, the crystallographic distortions that set in are by no means uniform. Even a sample that is a single crystal above the transition could have a multi-crystalline structure below the transition.

One must use two methods simultaneously in order to preserve the single-crystal structure of a sample of magnetite below the transition. The first aspect of the cooling procedure is that the sample must be cooled in a magnetic field of about one Tesla. The sample’s c^{*2} axis will align with the local magnetic field and magnetite is magnetically saturated when exposed to an external field of about 1 Tesla. Throughout the sample, the unit cells’ c^* axes will remain aligned with the magnetic field through the transition and will continue to remain aligned to each other when the

²Recall that for a unit cell described by vectors \mathbf{a} , \mathbf{b} , and \mathbf{c} , the c^* vector is the reciprocal lattice vector given by

$$\mathbf{c}^* = 2\pi \frac{\mathbf{a} \times \mathbf{b}}{\mathbf{a} \cdot \mathbf{b} \times \mathbf{c}}$$

which means it is perpendicular to the $\mathbf{a}-\mathbf{b}$ plane (Kittel, Introduction to Solid State Physics, seventh edition, 33). Having the c^* axes aligned means the $\mathbf{a}-\mathbf{b}$ planes are all parallel. Note that the c^* axis is only parallel to the \mathbf{c} axis when \mathbf{c} is orthogonal to \mathbf{a} and \mathbf{b} .

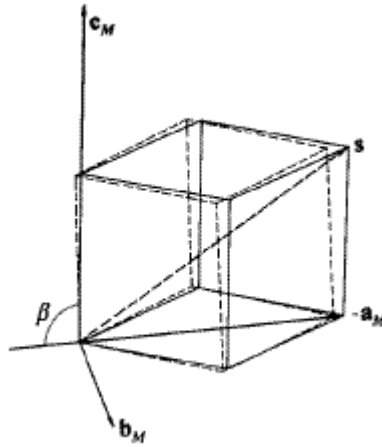


Figure 2: from [4]. This exaggerated diagram should give some idea of how the original cubic unit cell would be distorted into the low-temperature monoclinic structure. Note that the unit cell in the low- T phase is itself not a cube. The dashed lines indicate the original cube; the solid lines show the modified structure. The angle β is 90.2° , a 0.2° departure from the cubic angle.

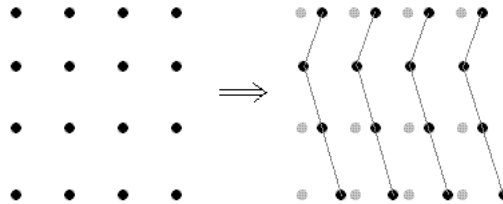


Figure 3: A cartoon picture of twinning due to a monoclinic distortion. The left-hand side is a cubic lattice; on the right-hand side, the gray dots indicate the original cubic positions and the black dots indicate the new cell positions. The twins meet at the second row from the top.

magnetic field is removed. After cooling through the transition and removing the field the sample must be mechanically de-twinned, which amounts to squeezing it. (One might reasonably expect the sample to crack under the strain of mechanical de-twinning, but this is not the case.) Iizumi and collaborators squeezed their sample around the $[1\ 1\ 1]$ direction, indicated by the vector \mathbf{S} .

If one fails to perform this complicated procedure, the results will at best apply only to polycrystalline magnetite. While this is useful information, the behavior of polycrystalline samples could vary significantly from that of a mono-crystalline sample.

2.3 Stoichiometry [10]

The iron-oxides are not limited to magnetite, Fe_3O_4 , but include wüstite, FeO , and hematite, Fe_2O_3 . Samples that are not carefully prepared could have wüstite and hematite impurities. This is especially true for natural crystals. For the formula unit $Fe_{3(1-\delta)}O_4$, δ values are limited to $-0.00006 < \delta < 0.0125$ before mixing with the other iron-oxides occurs.

Even for δ in the specified range, the variation in the thermodynamic character of the Verwey transition is significant. For pure magnetite, the transition is first order and the temperature of the transition is about 124 K. Any departures from purity will lower the transition temperature and for $\delta > 0.004$, the transition becomes second-order. In contrast, the heat-capacity data above

the transition indicates that the high-temperature behavior of magnetite is fairly insensitive to stoichiometry.

Kuipers and Brabers [11] studied the Seebeck effect for varying stoichiometry. The Seebeck effect is a fairly complex phenomenon³ and what it can indicate about a complicated phase transition is limited. Making the assumption that magnetite is a semiconductor in the low-temperature phase they found that the conduction charge carriers were a mixture of holes and electrons. The ratio of holes to electrons depended upon stoichiometry.

3 Theories Behind the Behavior

3.1 Hopping and Charge Ordering

Verwey's original hypothesis stated that we can think of the B sites as a pair of Fe^{3+} ions that happen to have an electron between the two of them. Conduction is then a matter of thermally activated electron hopping amongst adjacent Fe^{3+} sites. As we lower the temperature, the thermal fluctuations decrease until they are unable to overcome the hopping barrier. This occurs at the transition temperature, T_V . [3]

In order to put the theory on a more theoretical footing, one assumes that magnetite can be described by the Heisenberg model.[9] This model assumes interactions between the spins of nearest neighbor Iron ions as well as interactions with an external magnetic field.

Since the Iron ions occupy two distinct sites - A and B - the Hamiltonian will have three sums over nearest neighbors: AA, BB, and BA. The coefficients of the three possible neighbor pairs are called the *exchange integrals* and is notated J_{ij} where i and j are one of A and B.

One would expect the most sensible charge ordering to be that which minimizes the Coulomb repulsion between the hopping electrons, a situation known as the Anderson Condition [1]. Néel found exchange integrals showing that such charge ordering agreed with experimental data - particularly the heat capacity measurements - within an order of magnitude [12]. These calculations gave a solid theoretical confirmation for the charge ordering picture. Neutron scattering measurements made ten years later indicated reflections in the $[002]$ direction and confirmed the presence of charge ordering [13].

All of these models and calculations focused almost entirely upon explaining the transport measurements for which the phase transition was first known. The presence of the structural shift, discovered in the late 1950s and authoritatively documented in the 1970s and early 1980s introduced complications that could not be reconciled with the original charge ordering picture. The first conflict was that Verwey's charge ordering scheme rested upon the assumption that magnetite exhibited the same orthorhombic symmetry below the transition as above. The neutron measurements that initially seemed to confirm the charge ordering scheme were reproduced and the $[002]$ reflections were completely explained by other, simultaneous reflections. [4]

The heat capacity spike at the transition temperature should reflect all changes that take place in the phase transition. Néel's explanation of the heat capacity curve by electronic considerations alone, neglecting structural considerations, called his exchange integral calculations into question. Further doubt was shed upon the calculations and the theoretical footing of the charge ordering model when it was observed that the value of the exchange integrals can vary greatly with slight distortions of the atomic positions. [6]

Charge ordering is still a model that is pursued despite these objections. More recent work was performed by Wright *et al.* that indicated a different charge ordering scheme. Over four Iron sites, a

³For a simple introduction to the Seebeck effect, see http://en.wikipedia.org/wiki/Peltier-Seebeck_effect.

distinct arrangement of valences +2.4 and +2.6 were measured. The arrangements did not satisfy the Anderson condition (minimal electrostatic repulsion) but the authors explained the charge ordering by a charge density wave mechanism. Wright’s primary hypothesis was that the charge ordering caused differences in the $Fe - O$ bond lengths, and these differences led to the charge calculations by applying an method known as bond valence sums. [14] Further consideration of the accuracy of BVS calculations indicated that the variation in bond lengths was within experimental error [15]. Extensive study by McQueeney *et al.* shows that various charge ordering Hamiltonians do not satisfactorily explain the full system. [18]

3.2 LSDA+DMFT [8, 16]

The most recent calculations using the local spin density approximation along with dynamical mean field theory rest largely upon the Jahn-Teller effect. This effect describes how geometrical distortions can break otherwise degenerate electron states.

The basic premise involves the symmetries of the system. Any given molecule has a set of point symmetries for which it is invariant. The Hamiltonian must obey these symmetries and typically such symmetries arise in our consideration of the structure of the allowed electronic states. Various normal (vibrational) modes of the molecule also satisfy these symmetries. One then introduces interactions between the normal modes and the electronic states that share the same symmetries and includes them in the Hamiltonian. Although *a priori* explanations for the coupling may be elusive, such interactions serve the important role of differentiating two otherwise degenerate electronic states.

The Jahn-Teller effect makes use of the Born-Oppenheimer (adiabatic) approximation. We can conceptualize that approximation as constraining the system to a particular surface, called an adiabatic potential energy sheet (APES). Although we typically assume in the adiabatic approximation that the ground-state APES is separated from the next nearest APES by an appreciable energy gap, the Jahn-Teller effect arises when we discard that assumption and consider a collection of APESs that lie near each other (though far away from the remaining APES).

To put a more concrete flavor on all of this, consider two vibrational modes indexed by θ and ϵ , drawn figuratively in figure 3.2 on the following page. If we take a corresponding set of degenerate eigenkets $|\psi_\theta\rangle, |\psi_\epsilon\rangle$, and introduce the interaction according to the matrix $\begin{bmatrix} -Q_\theta & Q_\epsilon \\ Q_\epsilon & Q_\theta \end{bmatrix}$, then we see that the ϵ -mode tends to mix the two states whereas the θ -mode tends to keep the two modes distinct, splitting the degeneracy. We can diagonalize the the Hamiltonian after a suitable change of coordinates and arrive at two APESs, as in figure 3.2 on the next page. This system still has a continuum of degeneracies, so proceeding to nonlinear (cubic) Jahn-Teller interactions leads to a pair of APESs that breaks the degeneracy, shown in figure 3.2 on page 7.

The underlying theory of LSDA+DMFT is discussed in reference [17]. Craco and associates do not assume charge ordering nor do they assume simple overlap integrals as given by the exchange integrals used in a Heisenberg model. The details of their calculations are beyond the scope of this work (and its author) because the results in the form of spectral density functions, which do not have immediate comparison with recent experiment work. However, their calculations agree with other models, both above and below the transition, which have been compared with experimental studies. For this reason, these calculations show the greatest promise for giving a complete description of the Verwey transition.

4 Conclusion

The Verwey transition has been studied extensively since its inception, yet there is still no widely accepted theory explaining the phase transition. Despite initial wide acceptance of the explanation

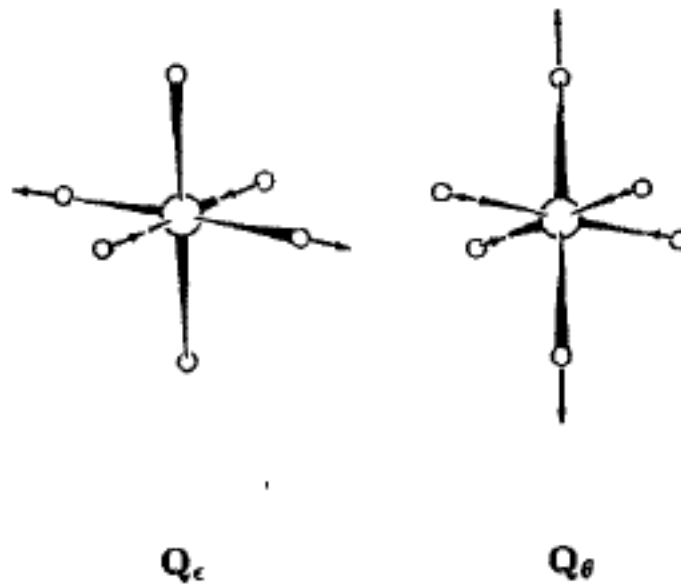


Figure 4: The two normal modes associated with the indices θ and ϵ .

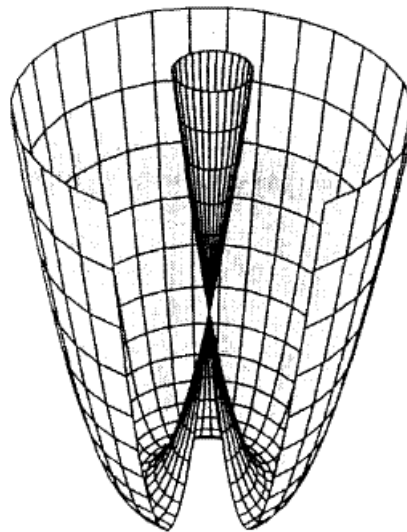


Figure 5: This is the pair of APESs for the two-mode system under consideration, called a “Mexican Hat” potential by the author. This looks almost exactly like the Landau free energy surface that led to the discussion of Goldstone modes.

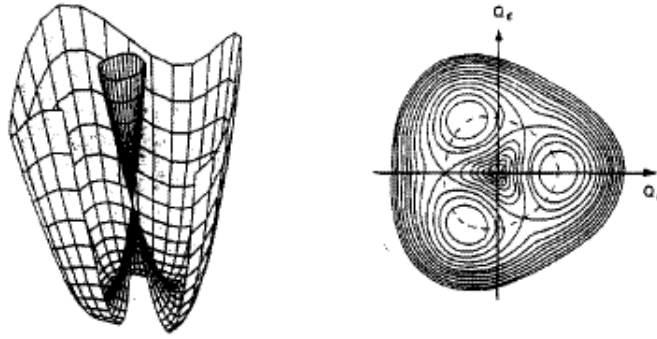


Figure 6: Warped Mexican Hat. This shows how cubic Jahn-Teller interactions can lead to distinct states in Q_ϵ and Q_θ space, breaking the electronic degeneracy.

that charge ordering of the A-site Iron ions, a great body of work indicates that such models are inadequate. A full explanation of Magnetite must take the structural deformations into account. Recent calculations considering the Jahn-Teller effect show the most potential for explaining this 70-year old problem.

References

- [1] W. Montfrooij, personal correspondence
- [2] E. J. W. Verwey, *Nature* **144**, 327 (1939)
- [3] E. J. W. Verwey, P. W. Haayman, F. C. Romeijan, *J. Chem. Phys.* **15**, 181 (1947)
- [4] M. Iizumi, T. F. Koetzle, G. Shirane, S. Chikazumi, M. Matsui, S. Todo, *Acta Cryst.* **B38**, 2121 (1982)
- [5] N. C. Toombs, H. P. Rooksby, *Acta Cryst.* **4**, 474 (1951)
- [6] J. Garcia, G. Subia, *J. Phys.: Condens. Matter* **16**, R145 (2004)
- [7] Z. Zhang, S. Satpathy, *Phys. Rev B* **44**, 13319 (1991)
- [8] L. Craco, M. S. Laad, E. Müller-Hartmann, cond-mat/0511930
- [9] M. L. Glasser, F. J. Milford, *Phys. Rev.* **130**, 1783 (1963)
- [10] J. P. Shepherd, J. W. Koenitzer, R. Aragón, J. Spalek, J. M. Honig, *Phys. Rev. B* **43**, 8461 (1991)
- [11] A. J. M. Kuipers, V. A. M. Brabers, *Phys. Rev. B* **14**, 1401 (1976)
- [12] L. Néel, *Ann. Phys.* **3**, 137 (1948)
- [13] W. C. Hamilton, *Phys. Rev.* **110**, 502 (1958)
- [14] J. P. Wright, J. P. Attfield, P. G. Radaelli, *Phys. Rev. Lett.* **87**, 266401 (2001)
- [15] J. Garcia, B. Subias, J. Blasco, M. G. Proietti, cond-mat/0211407
- [16] M. C. M. O'Brien, C. C. Chancey, *Am. J. Phys.* **61**, 688 (1993)
- [17] G. Kotliar, S. Y. Savrasov, K. Haule, V. S. Oudovenko, O. Parcollet, C. A. Marianetti, cond-mat/0511085
- [18] R. J. McQueeney, M. Yethiraj, W. Montfrooij, J. S. Gardner, P. Metcalf, J. Honig, cond-mat/0602214